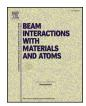
ELSEVIER

Contents lists available at ScienceDirect

Nuclear Inst. and Methods in Physics Research B

journal homepage: www.elsevier.com/locate/nimb



High-accuracy Geant4 simulation and semi-analytical modeling of nuclear resonance fluorescence



Jayson R. Vavrek*, Brian S. Henderson, Areg Danagoulian

Laboratory for Nuclear Security and Policy, Massachusetts Institute of Technology, 77 Massachusetts Avenue, Cambridge, MA 02139, USA

ARTICLE INFO

Keywords:
Nuclear resonance fluorescence
G4NRF
Geant4
Benchmarking
Verification

ABSTRACT

Nuclear resonance fluorescence (NRF) is a photonuclear interaction that enables highly isotope-specific measurements in both pure and applied physics scenarios. High-accuracy design and analysis of NRF measurements in complex geometries is aided by Monte Carlo simulations of photon physics and transport, motivating Jordan and Warren (2007) to develop the G4NRF codebase for NRF simulation in Geant4. In this work, we enhance the physics accuracy of the G4NRF code and perform improved benchmarking simulations. The NRF cross section calculation in G4NRF, previously a Gaussian approximation, has been replaced with a full numerical integration for improved accuracy in thick-target scenarios. A high-accuracy semi-analytical model of expected NRF count rates in a typical NRF measurement is then constructed and compared against G4NRF simulations for both simple homogeneous and more complex heterogeneous geometries. Agreement between rates predicted by the semi-analytical model and G4NRF simulation is found at a level of $\sim 1\%$ in simple test cases and $\sim 3\%$ in more realistic scenarios, improving upon the $\sim 20\%$ level of the initial benchmarking study and establishing a highly-accurate NRF framework for Geant4.

1. Introduction

In recent years, nuclear resonance fluorescence (NRF)—the resonant absorption and re-emission of photons by a nucleus—has been widely-proposed as a powerful isotope-specific assay technique. Nuclear weapon treaty verification [1,2], spent fuel measurement [3], and cargo scanning [4,5] systems use NRF as an active interrogation technique to discern the isotopics of or detect the presence and quantity of special nuclear materials. In the domain of pure physics, NRF is useful as a probe of nuclear structure across a broad array of isotopes [6].

For realistic experimental geometries, expected NRF count rates may be calculated through Monte Carlo simulation of photon and electron transport and physics. The G4NRF [7] package for the Geant4 [8] Monte Carlo toolkit was developed by Jordan and Warren at Pacific Northwest National Laboratory, while NRF data libraries for MCNPX [9] have been developed by Wilcox et al. at Los Alamos National Laboratory [10]. In the former case, NRF rates predicted by the G4NRF code were initially only benchmarked against theory to within $\sim 20\%$ and validated against data to within a factor of ~ 3 [11]. Moreover, the initial study made a number of mathematical simplifications in its analytical model: it neglected non-resonant photon attenuation (e.g., Compton scattering), assumed the emission of NRF photons to be

isotropic, and implemented a Gaussian approximation to the NRF cross section that is not valid for thick targets or large resonance widths. This benchmarking study accounts for these three effects and therefore presents improved benchmarking of the G4NRF code against a more accurate semi-analytical radiation transport model. To this end, Section 2 first constructs this high-accuracy semi-analytical model for the NRF photon count rate observed by a detector. A series of Geant4 + G4NRF Monte Carlo simulations is then compared against the semi-analytical model in Section 3. Section 4 concludes with a discussion of results.

2. Semi-analytical model for NRF count rates

In this section we present a model for predicting the absolute NRF count rate observed by a detector in a transmission NRF measurement. The model is based upon the NRF cross section and radiation transport development previously given in the literature (primarily Refs. [12,13]), but expands the treatment to multiple-isotope targets and practical considerations for high-accuracy computation. First, we derive the NRF cross section necessary for both the semi-analytical and G4NRF rate predictions. We will then show that the shape of the NRF cross section can influence NRF count rate predictions substantially for thick targets, motivating the derivation and use of highly accurate cross

E-mail addresses: jvavrek@mit.edu (J.R. Vavrek), bhender1@mit.edu (B.S. Henderson), aregjan@mit.edu (A. Danagoulian).

^{*} Corresponding author.

section formulae. We then apply the NRF cross section to the radiation transport problem that describes a generic transmission NRF measurement in order to construct a semi-analytical model for the expected NRF count rate. Such semi-analytical calculations necessarily involve approximations to keep the mathematics tractable, and thus are somewhat limited in the experimental complexity they can accurately model. However, they offer a powerful tool for investigating the dependence of NRF count rates on various physics or geometrical parameters without running computationally expensive simulations, and are useful in verifying the implementation and accuracy of the G4NRF code.

2.1. NRF cross sections

Nuclear resonance fluorescence (NRF) describes the $X(\gamma, \gamma')X$ reaction in which a nucleus X with resonance energy E_r resonantly absorbs a photon of energy $E \simeq E_r$, thereby transitioning from its ground state to the excited state at E_r [6,12]. The excited nucleus subsequently decays after time $\mathcal{O}(fs)$, re-emitting a photon of energy $E' \simeq E$ (neglecting the relatively small nuclear recoil given later in Eq. (10)) if the decay is direct to the ground state, or a lower energy $E' \simeq E - E_j$ if the decay proceeds first through an intermediate level j.

The NRF cross section (at temperature T = 0 K) for absorption through an isolated resonance at energy level E_r followed by decay to an energy level E_j may be found (using, e.g., perturbation theory [14]) to follow a single-level Breit-Wigner profile [12]:

$$\sigma_{r,j;0K}^{NRF}(E) = \pi g_r \left(\frac{\hbar c}{E}\right)^2 \frac{\Gamma_{r,0}\Gamma_{r,j}}{(E - E_r)^2 + (\Gamma_r/2)^2}.$$
 (1)

The g_r term is a statistical factor arising from the number of available nuclear spin and photon polarization states, given by

$$g_r = \frac{2J_r + 1}{2(2J_0 + 1)},\tag{2}$$

where J_0 and J_r are the ground-state and resonant-level nuclear spins, respectively. The $\Gamma_{r,0}$ and $\Gamma_{r,j}$ terms denote the partial widths for decay from the level at E_r to E_j , while the Γ_r is the total width of the level, i.e., the sum of the partial widths. For most calculations in this work, it is more convenient to work with the cross section for absorption only,

$$\sigma_{r;0K}^{\rm NRF}(E) = \sum_{j} \sigma_{r,j;0K}^{\rm NRF}(E) = \pi g_r \left(\frac{\hbar c}{E}\right)^2 \frac{\Gamma_{r,0}\Gamma_r}{(E - E_r)^2 + (\Gamma_r/2)^2},$$
(3)

which differs from the absorption + decay cross section only by the level's branching ratio $b_{r,j} \equiv \Gamma_{r,j}/\Gamma_r$, with the normalization condition $\sum_j \Gamma_{r,j} = \Gamma_r$, i.e., $\sum_j b_{r,j} = 1$.

At non-zero temperatures, the NRF absorption cross section is most accurately described by a Doppler-broadened version of the Breit-Wigner distribution in Eq. (3):

$$\sigma_r^{\text{NRF}}(E) = 2\pi^{1/2} g_r \left(\frac{\hbar c}{E_r}\right)^2 \frac{b_{r,0}}{\sqrt{t}} \int_{-\infty}^{+\infty} \exp\left[-\frac{(x-y)^2}{4t}\right] \frac{dy}{1+y^2},\tag{4}$$

which integrates over the thermal distribution of speeds of the target nuclei [12]. Here we have suppressed the temperature subscript for brevity, replaced the $1/E^2$ term with $1/E_r^2$ (valid near the resonance), and defined

$$x \equiv 2(E - E_r)/\Gamma_r,\tag{5}$$

$$t \equiv (\Delta/\Gamma_r)^2,\tag{6}$$

where is the width of the level after Doppler broadening, with

$$\Delta = E\sqrt{\frac{2kT}{Mc^2}},\tag{7}$$

where k is Boltzmann's constant, T is the absolute temperature, and Mc^2

is the rest-mass energy of the nucleus. ¹The NRF cross section given by Eq. (4) is implemented in both the semi-analytical NRF rate model in the next section and the G4NRF Monte Carlo code.

A useful measure of the 'strength' of a resonance is the integrated cross section.

$$\int \sigma_r^{\text{NRF}}(E) dE = 2\pi^2 g_r \left(\frac{\hbar c}{E_r}\right)^2 \Gamma_{r,0},\tag{9}$$

which can be found by approximating $(\hbar c/E)^2 \simeq (\hbar c/E_r)^2$ and $E_r \gg \Gamma_r$ then integrating Eq. (3) over $E \in [0, \infty)$, or by approximating $\Delta \simeq E_r \sqrt{2kT/Mc^2} \gg \Gamma_r$ then integrating Eq. (4) over $x \in (-\infty, \infty)$. As will be shown later, the expected NRF count rate in an experiment is proportional to the integrated cross section in the thin-target limit.

The fundamental parameters required in Eq. (4)—and thus determined for each resonant level in an NRF cross section measurement—are the level's width Γ_r and set of branching ratios $b_{r,i}$. The NRF transitions studied in this work are all transitions directly to the ground state, such that only the branching ratios to the ground state $b_{r,0}$ are necessary. Cross section parameters reported by different experiments (or tabulated in the ENSDF databases, e.g., Ref. [15]) can vary drastically, however. The ground-state branching ratio of the U-238 2.245 MeV level, e.g., differs by $\sim 30\%$ between ENSDF and Ref. [3], while its width Γ_r differs by more than an order of magnitude. Similarly, the values of $\Gamma_{r,0}^2/\Gamma_r$ reported by Ref. [3] and Ref. [16] differ by $\sim 25\%$ in the U-238 2.209 MeV line, and by a factor of 6 in the U-238 2.468 MeV line. These discrepancies may introduce systematic uncertainties much larger than our desired accuracy for the verification study; for consistency, then, both the calculations and simulations in this work use an assumed set of cross section parameters (in isotopes relevant to nuclear security applications—see Refs. [1,2]) from various references as shown in Table 1. For the U-238 resonances, preference is given to experimentally-determined (i.e., not ENSDF-evaluated) data; specifically, the integrated cross sections and ratios of widths in Table 1 of Ref. [3] (which derive from Ref. [17]) are used to infer values of Γ_r and $b_{r,0}$ for the three major U-238 resonances. No NRF data on Pu-240 exists in ENSDF, so values of Γ_r and $b_{r,0}$ are similarly inferred from experimental data in Table II of Ref. [18]. For the 2.212 MeV resonance of Al-27, the value of Γ_r is determined from the lifetime listed in Table 27.4 of Ref. [19] and $b_{r,0}$ is found using Table 27.6 of the same work. We note that while some of the U-238 cross section parameters may vary significantly across references, the Al-27 parameters generally agree to within a few percent. Since the Γ_r and $b_{r,0}$ values read by G4NRF are stored in plaintext files, the user may configure G4NRF to use a custom set of cross section parameters.

Due to conservation of energy and momentum, a free nucleus undergoing NRF will recoil with kinetic energy $E_{\rm rec}$ determined by the Compton-like formula

$$E_{\rm rec} = E \left[1 - \frac{1}{1 + E(1 - \cos\chi)/Mc^2} \right] \simeq \frac{E^2}{Mc^2} (1 - \cos\chi),$$
 (10)

where χ is the photon scattering angle relative to its incident direction, and $E \ll Mc^2$ has been applied in the Taylor expansion. For nuclei bound in an atomic lattice, $E_{\rm rec}$ may be large enough to overcome the lattice displacement energy $E_d \ (\gtrsim 10 \ {\rm eV}$ in pure metals [20]) in which case the kinetic energy transfer is $E_{\rm rec}$ – E_d . If the value of $E_{\rm rec}$ for an

$$T_{\text{eff}} = 3T \left(\frac{T}{\theta_D}\right)^3 \int_0^{\theta_D/T} x^3 \left(\frac{1}{e^x - 1} + \frac{1}{2}\right) dx,$$
 (8)

where the absorber's Debye temperature θ_D accounts for the effect of the atomic lattice on the ideal Maxwell-Boltzmann distribution of speeds. This change propagates through to the Δ of Eq. (7) and thus the t of Eq. (4). G4NRF uses $T_{\rm eff}$ if θ_D is known, and defaults to $T=300~{\rm K}$ otherwise.

 $^{^{1}}$ For greater accuracy, the temperature T may be replaced by the 'effective' temperature [12]

Download English Version:

https://daneshyari.com/en/article/8039022

Download Persian Version:

https://daneshyari.com/article/8039022

Daneshyari.com